Structures 68 (2024) 107044

Contents lists available at ScienceDirect

Structures

journal homepage: www.elsevier.com/locate/structures

Characterization of different longitudinal shear transfer mechanisms for profiles embedded in concrete walls

Dan Dragan [a], Rajarshi Das [a,*], Teodora Bogdan [b], Herve Degee [a]

[a] Construction Engineering Research Group, Hasselt University, Hasselt, Belgium
[b] ArcelorMittal Chair of Steel and Façade Engineering, FSTC, RUES, University of Luxembourg, Luxembourg

ARTICLE INFO

Keywords:
Steel-concrete composite construction
Steel profiles encased in concrete
Longitudinal shear transfer
Bond resistance
Steel plate connectors
Shear stud connectors

ABSTRACT

Concrete walls or columns reinforced by one or multiple embedded steel profiles have gained popularity due to their improved strength, ductility and energy dissipation capacity. However, certain gaps in information are remaining in the available standards regarding the design of such non-conventional reinforced concrete systems. In particular, a proper characterization of the longitudinal shear transfer properties at the steel-concrete interface is required for a reliable design. Although sufficient information is available regarding mechanical connectors like shear studs, detailed information is required for any other types of mechanical connectors such as welded steel plates or for configuration without mechanical connectors. Moreover, even for cases with mechanical connectors, the orientation of the profile – and hence the distance to the face of the concrete – and the tying system can have a significant influence on the load transfer mechanisms. To this purpose, this article presents the outcomes of a set of push-out tests with the objective of comparing the force transfer mechanisms from the steel profile to the surrounding concrete wall for different types of interfaces. 13 tests specimens are investigated, with flexible (shear studs) and/or rigid (steel plates) shear connectors, considering different orientations of the profile and tying mechanisms, as well as a comparison with profiles without mechanical connectors. Based on the test results and subsequent analytical assessment, relevant conclusions are drawn regarding the longitudinal shear transfer at the steel-concrete interface. If necessary provisions are followed, welded steel plates prove to be an effective alternative to the shear stud connectors in terms of connector strength. The orientation of the embedded steel profile, consequent position of the mechanical connectors and their distance to the concrete face are observed to have a significant influence on the compression strut evolution, which therefore dictates the necessity (or not) of horizontal confinement or ties. Furthermore, combining the shear strength offered by different types of mechanical connectors and the steel-concrete bond offer a precise estimate of the longitudinal shear strength and therefore indicates towards the conservative nature of the design provisions suggested by the available standards.

1. Introduction

Steel-concrete composite sections, consisting of one or multiple steel profiles encased within a concrete member, have gained significant popularity in the last decade. They offer several advantages, such as: (1) a composite action, which increases the compression, bending and shear strength of the members and therefore reduces their required cross-section area compared to a classical reinforced concrete (RC) member; (2) an increased deformation capacity and energy dissipation, which improve the structure's performance against earthquakes; (3) larger weak axis stiffness, which eventually delays the possible out-of-plane buckling failure; and (4) an easier connection with steel and composite concrete floor beams thanks to the encased profiles. Significant numerical and experimental investigations have been dedicated to studying the behavior of such composite members, e.g. [1–7]. Design provisions have been developed and further documented in some leading design codes: AISC 341–10 [8], Eurocode 4 and 8 [9,13] and JGJ 3–2010 [10]. However, when it comes to the force transfer mechanism at the steel-concrete interface, there is a prevalent knowledge gap regarding certain aspects of a composite specimen, such as: (i) positioning of the connectors with respect to the faces of the concrete element (distance, orientation…), (ii) influence of concrete confinement

* Correspondence to: Universiteit Hasselt - Campus Diepenbeek, Kantoor ACB^2 1.4, Applicatiecentrum beton en bouw, Wetenschapspark 34, 3590, Belgium.
E-mail address: rajarshi.das@uhasselt.be (R. Das).

https://doi.org/10.1016/j.istruc.2024.107044
Received 8 January 2024; Received in revised form 26 June 2024; Accepted 6 August 2024
Available online 19 August 2024

around the profile, (iii) necessity of horizontal ties, (iv) possibility to combine different types of shear transfer mechanism. These aspects serve as the primary objectives of this research.

One of the main concerns in designing composite sections has always been the correct evaluation of the shear force – transferred at the steel-concrete interface or the connection zone. The shear force at the connection zone between the steel and the concrete components is fundamentally transferred by three mechanisms: a) chemical bonding: bond between the cement paste and the surface of the steel; b) friction: assumed proportional to the normal force at the interface; and c) mechanical connectors: providing the required interaction via embossments, ribs, shear studs or welded steel plates. The chemical bonding is basically a bond resistance which does not accompany slip. It is often sensitive to the applied load and is generally neglected in design and analysis [11] because, if and when the mechanical and frictional shear resistance is substantially lower than the initial shear resistance of the chemical bond, a brittle behavior is observed. In 1993, Daniels and Crisinel [12] documented a qualitative shear resistance versus slip behavior where both the "ductile" and the "brittle" behaviours were distinguished. The authors highlighted the fact that a brittle behaviour is typically associated with decking, considering small or no embossments, and without shear studs. Friction, on the other hand, is a shear resistance which exists even if there is slippage. Hence, the shear resistance due to friction alone is considered while designing and analyzing composite members. When it comes to the chemical bonding and friction, Eurocode 4 [13] provides some basic provisions to calculate and subsequently control the resistance to longitudinal shear at the steel-concrete interface, although quite limited. Finally, mechanical interaction offers a shear resistance which exists for both, stiff connectors (little or no slippage) and flexible connectors (higher slippage). Such shear connectors between a concrete member and a steel section provide the required composite action in flexure. They can also be used to distribute the large horizontal inertial forces in the slab to the main lateral load resisting elements of the structure [14] or to simply enhance the connection between the concrete and the steel elements. The type of shear connection used at the steel-concrete interface has a significant effect on the behavior of the composite member. Headed shear studs (flexible connectors) are usually welded to the steel beam to provide different degrees of connection between the concrete member and the embedded steel profile. Rigid/stiff shear connectors, such as steel plates, usually develop full composite action, whereas, flexible shear connectors generally develop a partial composite action. Therefore, the analysis procedure requires consideration of interlayer slip between the components. When shear studs are used, the bond stresses associated with these mechanical devices are much higher than the chemical bond stresses and the response is ductile [12]. In both cases however, the initial chemical bond associated with no slip is neglected in design and analysis [12]. The shear force transfer in composite members is experimentally measured using different techniques, among which, push-out tests have been the most common approach due to its simplicity [15–19].

In today's construction industry, different types of "shear connectors" are used to transfer the shear forces from a steel member to its surrounding concrete, e.g. headed shear studs, perfobond ribs, T-rib connectors, etc. Though, over the last 60 years, the headed shear studs have gained the maximum popularity. One of the most illustrated models to explain the load transfer of stud connectors in solid slab applications was given by Lungershausen [20] where four different components, which contribute to the total capacity of the connector, were defined (Fig. 1). Thanks to the extensive studies done by several other researchers [21–23], the load-transfer behaviour of the shear studs can now be efficiently predicted. As a result, standard design procedures have been documented in the structural codes all around the world and Eurocode 4 is no exception.

Nevertheless, the present versions of the structural codes offer little information when it comes to other types of shear connectors. A practical design tool to correctly estimate the shear resistance due to, for instance, stiffeners between the flanges of H-section (stiff connectors) is clearly missing. Although few researchers [24–27] in the past have studied the bond properties between a steel plate and concrete, and have subsequently categorized several types of failure mechanisms, the applicability of such stiffening plates as mechanical connectors remains unexplored. This study attempts to investigate the shear-force transfer behaviour of such welded steel plates and their efficiency to work as shear connectors with respect to a recently developed design approach [29].

This article presents the analytical and experimental investigations conducted on the shear transfer between an embedded profile and a surrounding concrete block developed in the frame of an EU-RFCS research project - "Smartcoco" (Smart Composite Components) [28]. A rectangular cross-section is specifically chosen for the concrete block in order to investigate the influence of the orientation of the steel profile, and therefore the distance from the embedded steel to the concrete face, with the view of using the outcomes to design the profiles as embedded reinforcements in walls (see Fig. 2). Practical examples of such a technical solution can be found in chapter 1 of Ref. [29]. Different horizontal confinement schemes (i.e. stirrups, ties and hoops) are investigated, as well as different types of shear connections at the steel-concrete interface, such as: (i) flexible shear stud connectors, (ii) stiff steel plate connectors and (iii) steel-concrete bond without mechanical connectors. Push out tests are performed. The primary objective is to characterize the different longitudinal shear-transfer mechanism at the steel-concrete interface by: (1) checking the shear stud behaviour based on the Eurocode 4 provisions to have a reference configuration, (2) analysing and comparing the welded plates' behaviour with the stud connectors and then validating a recently developed design method for the welded plate connectors [29], (3) investigating the influence of the embedded profile's orientation and the horizontal confinement, (4) assessing the design feasibility to combine multiple types of shear connectors and (5) validating the design shear (bond) strength values recommended by

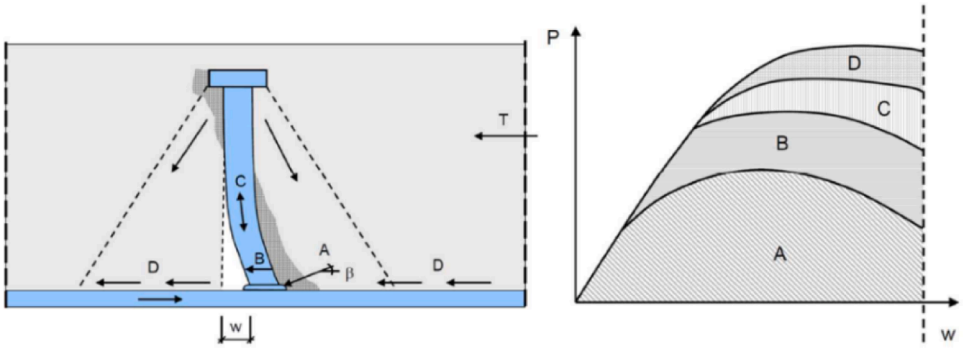

Fig. 1. Load transfer of a headed stud connector in a solid slab in accordance with Lungershausen [20].

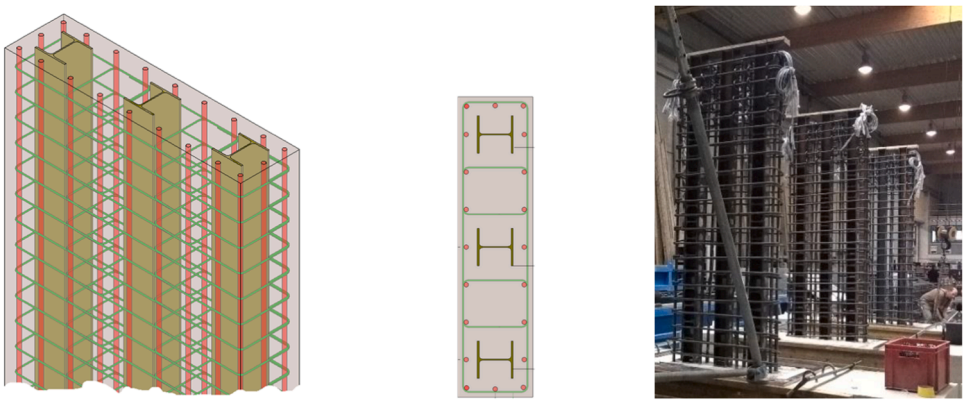

Fig. 2. Examples of concrete walls reinforced with several encased steel profiles.

Eurocode 4 Table 6.6 [13] at the steel-concrete interface in the absence of mechanical connectors and the possibility to superimpose the bond resistance and the resistance from the mechanical connectors.

2. Experiments – general assumptions, test specimens, set-up and instrumentation

Section 2.1 describes the geometric properties of the test specimens with different types of shear connectors, corresponding vertical and horizontal reinforcement schemes, different orientations and surface finishing of the embedded steel profiles, using schematic diagrams. Section 2.2 summarizes the material properties obtained from cube compression tests and steel coupon tests. The test set-up and instrumentation are presented in Section 2.3.

2.1. Description of the test specimens

Certain parameters are kept constant for all configurations such as: the embedded profile is chosen to be a HEB120 section (h_{HEB120} = 120 mm and b_{HEB120} = 120 mm); the wallet thickness is estimated as $B_{wall} = 2\ c_v + 2\phi_1 + h_{HEB120} + 2h_{sc} = 340$ mm, where c_v is the concrete cover = 35 mm, Φ_l is the diameter of the longitudinal reinforcement = 10 mm and h_{sc} is the shear stud height = 65 mm. The height (H_{wall}) and depth (D_{wall}) of the RC wallets are respectively 450 mm and 1000 mm for configurations A-E, whereas, for configurations F and G, both the height (H_{wall}) and depth (D_{wall}) are 1000 mm. Higher wallets are considered for configurations F and G to have a better distribution of the friction resistance along the embedded steel profile, which is not necessary for the other specimens due to the more discrete shear transfer mechanism provided by the mechanical connectors. 6Φ10 vertical rebars are provided on each side of the wallets with a spacing of 185 mm as per Eurocode 2 [30].

1. **Configuration A:** *3 flexible shear stud connectors* are adopted on each side of the profile with the corresponding geometrical properties: stud diameter, d = 16 mm; stud height, h_{sc} = 65 mm, longitudinal spacing, s_c = 150 mm. The HEB120 profile is embedded with its *strong axis perpendicular to the longer wall face.* Conventional horizontal reinforcements are first provided (3Φ12 stirrups on each side of the wall at a distance of s_c = 150 mm). However, due to the orientation of the steel profile, 3Φ12 transverse links are also provided (under each connector) to transfer the compression struts from the studs to the vertical rebars (see Fig. 3), according to Eurocode 4 recommendations. A single test is performed on this configuration to validate the provisions of Eurocode 4.
2. **Configuration B:** *2 stiff welded plate connectors* are adopted on each side of the embedded profile with the following geometric properties: width = 56.75 mm, length = 98 mm, thickness = 9 mm and spacing, s_p = 250 mm. The HEB120 profile is embedded with its *strong axis perpendicular to the longer wall face*. Three different horizontal tying schemes (see Fig. 4) are tested for this configuration to study the influence of tying and concrete confinement: (i) only

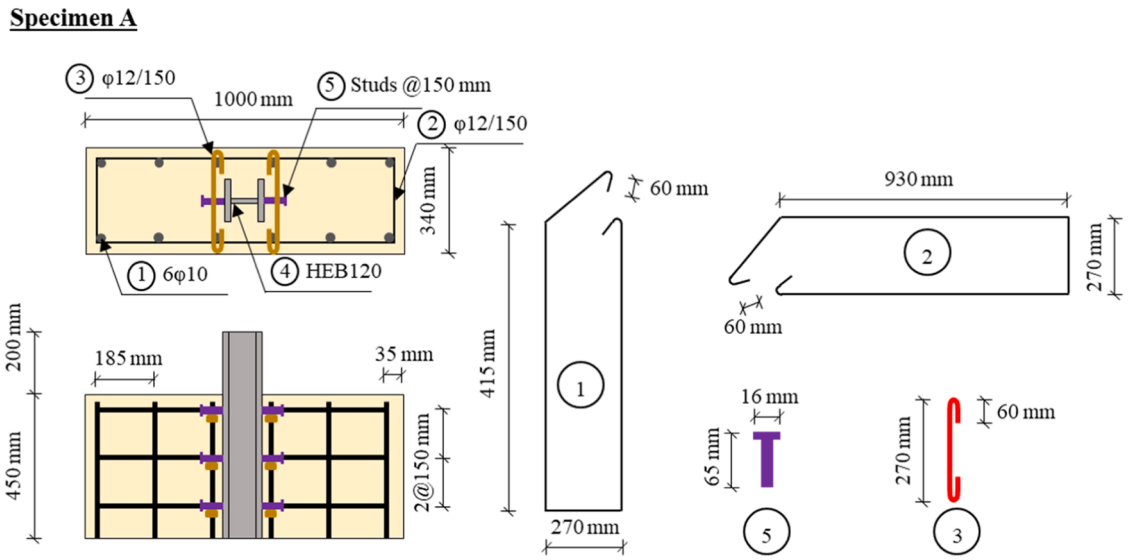

Fig. 3. Configuration A - cross-section detailing.

conventional stirrups are provided in Specimen B1, (ii) 3Φ12 additional horizontal hoops are placed with a spacing of 125 mm in Specimen B2, (iii) 3Φ12 additional horizontal links are placed at each side of the wall with a spacing of 250 mm in Specimen B3.

3. **Configuration C:** *3 flexible shear stud connectors* are used on each side of the embedded steel profile (Fig. 5). The HEB120 profile is embedded with its *strong axis parallel to the longer wall face.* The geometric properties of the shear studs, vertical reinforcements and horizontal reinforcements are kept the same as adopted for Configuration A. Additional transverse links are not required in this case because of the presence of the overall stirrups in the wall. Only one specimen is tested and then compared with Configuration A, in order to understand the influence of the orientation of the steel profile with its consequences of the distance between the profile and the concrete face.

Configuration D: *2 stiff welded plate connectors* are adopted on each side of the embedded steel profile. The HEB120 is embedded with its *strong axis parallel to the longer wall face.* The geometric properties of the plate connectors and vertical reinforcements are kept the same as adopted for Configuration B. Two different horizontal reinforcement schemes are adopted (see Fig. 6): (i) only conventional stirrups are provided in Specimen D1, (ii) 3Φ12 additional horizontal hoops and 3Φ12 additional horizontal links are provided in Specimen D2 at a distance of 125 mm. This configuration provides: (a) added information on the feasibility of plate connectors, (b) more details about the influence of the orientation of the steel profile and (c) horizontal confinement.

4. **Configuration E:** A combination of mechanical connectors is used – *1 flexible connector (stud) on the flange and 1 stiff connector (plates) between the flanges* – on each side of the profile. The HEB120 is embedded with its *strong axis parallel to the longer wall face.* 3Φ14 horizontal hoops and 3Φ14 transverse links are placed on each side of the wallets at a distance of 170 mm along with conventional horizontal stirrups (see Fig. 7). A single test is conducted in this case to assess and subsequently characterize the combined behaviour of flexible and stiff connectors while transmitting the applied forces from the steel profile to the concrete wall.
5. **Configuration F and G:** No mechanical connectors are used in these two configurations. The HEB120 steel profile is embedded with its *strong axis perpendicular to the longer wall face* (Fig. 8). The surface of the embedded profiles is **artificially rusted in Configuration F** and **painted in Configuration G** to cover the two extreme conditions at the steel-concrete interface and investigate them with respect to the design shear (bond) strength suggested by Table 6.6 of Eurocode 4.

Additional push-out test results (conducted in the frame of a separate research program) were recently published by the same authors [31] on square composite cross-sections (400 mm × 400 mm) with different force-transfer mechanisms at the steel-concrete interface. However, the reference configuration in that particular study consisted of a classically finished HEB200 steel profile without any mechanical connectors, embedded through 650 mm inside a 800 mm high wallet (see Fig. 9). 4φ16 longitudinal rebars were adopted with a concrete cover of 25 mm, and φ8 transverse stirrups were used at a spacing of 150 mm. 3 specimens were tested for this reference configuration. The corresponding results for the bond strength obtained from this classical solution with a normal surface finishing (named as **Configuration H** in this article) are also included in this study for the sake of comparison with configurations F and G.

2.2. Material properties

Compression tests are conducted on 150 mm × 150 mm x 150 mm concrete cubes. The average measured compressive strength is obtained as, $f_{c,\ exp} = 71$ MPa. The steel material properties (see Table 1) for the embedded profiles and the plate connectors are obtained from tensile tests done at the Department of Advanced Materials and Structures, Luxembourg, on rectangular coupons at ambient temperature according to EN ISO 6892–1 standard. The shear studs are however not tested explicitly and a declared strength was obtained from the manufacturer, i.e. tensile strength of one stud, $f_u = 450$ MPa. The material strength properties for the analytical assessment of the tested configurations (discussed in Section 3.2) are chosen accordingly, i.e. $f_{c,\ exp} = 71$ MPa, $f_{ay} = 460$ MPa and $f_u = 450$ MPa. The mean elastic modulus values are adopted for the concrete and steel material, respectively as $E_{cm} = 35000$ MPa and $E_a = 210000$ MPa. A S500 steel (declared yield strength, $f_{sd} = 500$ MPa) with an elastic modulus, $E_s = 200000$ MPa is adopted for the rebars following the production specifications.

2.3. Preparing specimens, test set-up and instrumentation

The specimens are prepared and casted horizontally (Figs. 10 and 11) with utmost care to position correctly the profile within the formwork and achieve a suitable bond between the embedded steel profile and the surrounding concrete. A relatively higher slump concrete (S3 – S4) should be used with smaller aggregate size (20 mm) in order to avoid water bubbles and simultaneously obtain a dense concrete underneath the mechanical connectors, especially the welded steel plates. As illustrated in Section 2.1, concrete is casted all around the embedded profiles to characterize the global behaviour of the steel-concrete interface for fully embedded profiles including all contributions, i.e. shear connectors

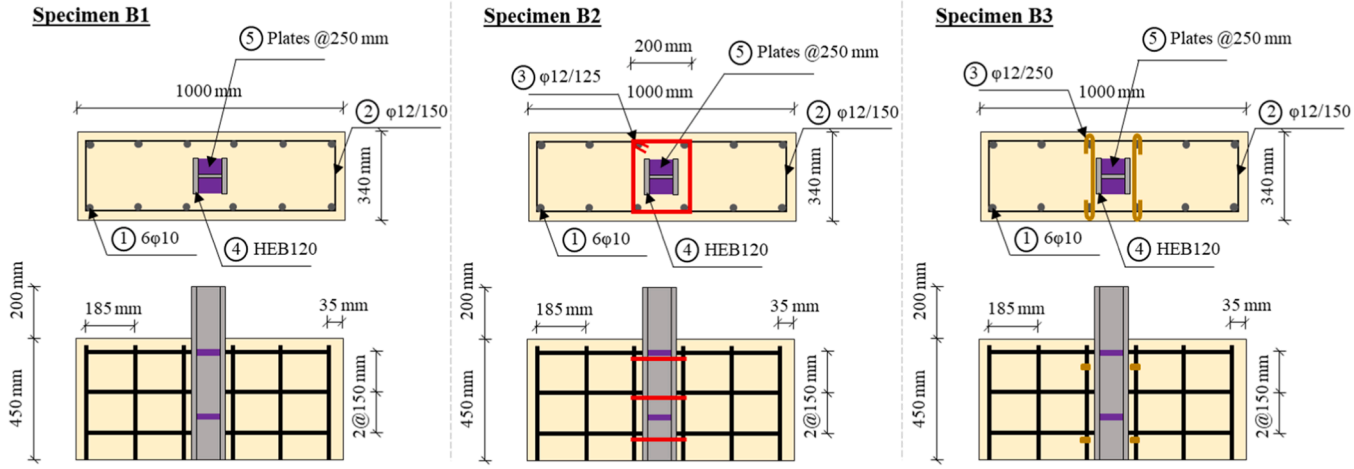

Fig. 4. Configuration B - cross-section detailing.

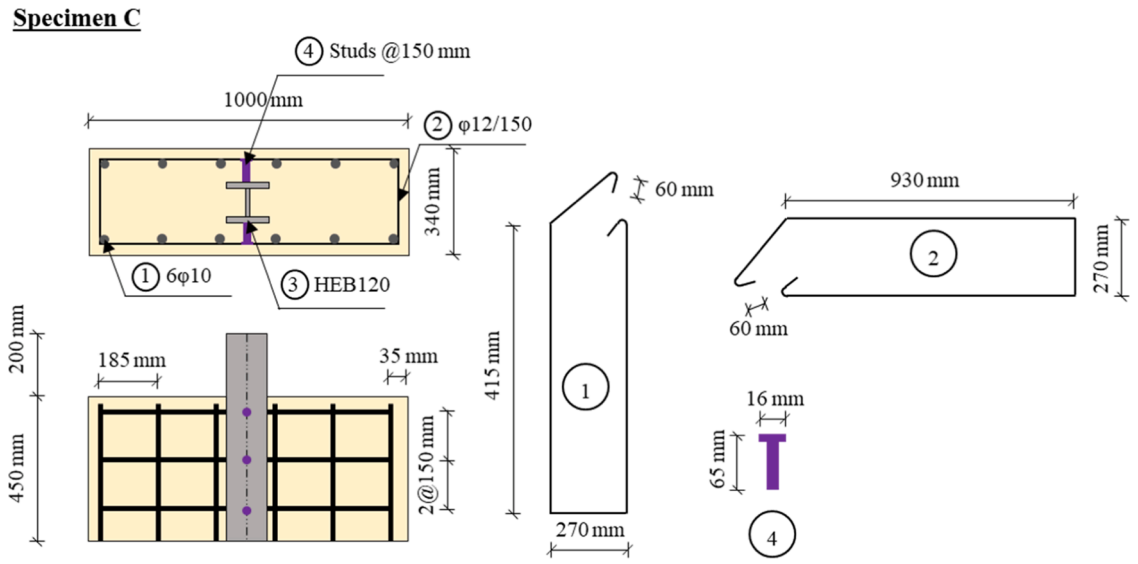

Fig. 5. Configuration C - cross-section detailing.

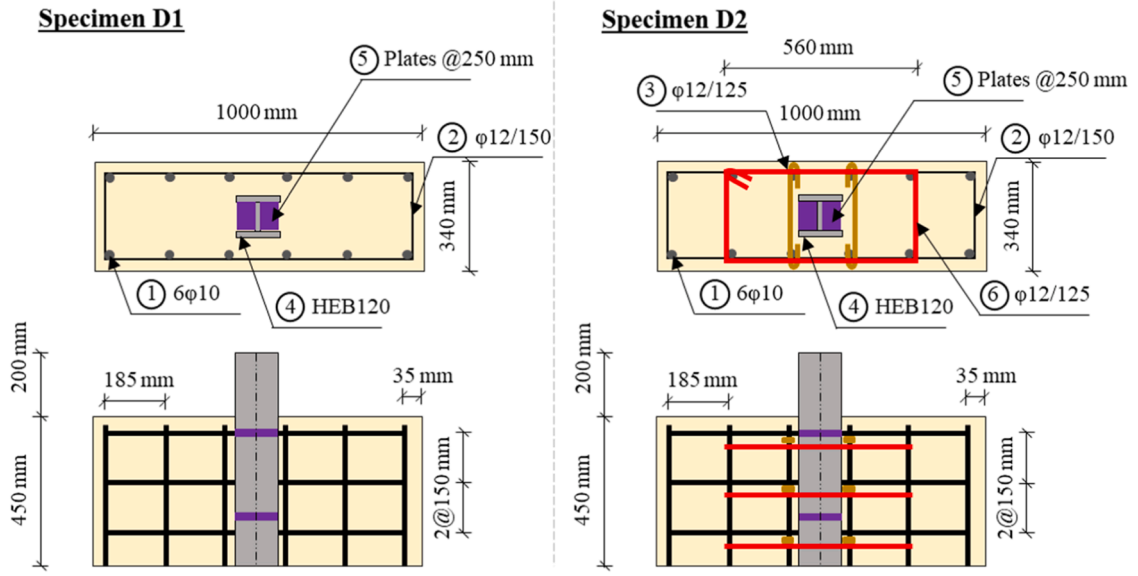

Fig. 6. Configuration D - cross-section detailing.

and bond. Push-out tests are performed at the Material & Structures Laboratory of the University of Liège. Fig. 11 shows a schematic diagram with an image of the actual test set-up, supports and load application. The vertical load is applied on a steel end plate resting on the top of the profile. The end-plate is not welded to the profile to ensure a full load transfer only via longitudinal shear. As the width of the concrete part on either side of the encased steel is significantly wider than the steel profile, supporting the full base of the concrete parts can lead to global arching effects, which can increase the friction at the steel-concrete interface and provide an overestimated value for the steel-concrete bond strength. In order to avoid such a scenario, only a part of the concrete base is supported by two H-profiles (Fig. 11b), clamped to 160 mm wide plates (Fig. 11c). The out of plane deformation of the wallets are restricted. 4 displacement transducers are used – 2 at the top of the wallet (one at each side of the profile), 1 at the top and 1 at the bottom of the profile to obtain the vertical displacements. Furthermore, 6 strain gauges are placed @ 150 mm along the length of the embedded profile for configurations F and G, to obtain the bond stress evolution at the steel-concrete interface. The first strain gauge is placed at a distance of 90 mm from the top of the wallet. 1 load cell is positioned at the top of the steel profile.

3. Results and discussions

The push-out test results as well as the analytical assessment are discussed. First, a global overview is presented to summarize the experimental outcomes for all specimens in terms of load-displacement behavior, resistances obtained at relevant points and crack patterns. Then, the analytical resistances are estimated and compared with the experimental values. Finally, the influence of different parameters is discussed: (i) the orientation of the steel profile and position of the connectors with respect to the faces, (ii) efficiency of the welded steel plate connectors, (iii) horizontal tying and confinement, (iv) combination of different types of mechanical connectors and (v) different surface conditions at the steel-concrete interface. The displacement values plotted in the subsequent figures correspond to the data obtained from the displacement transducer located at the bottom of the steel profile.

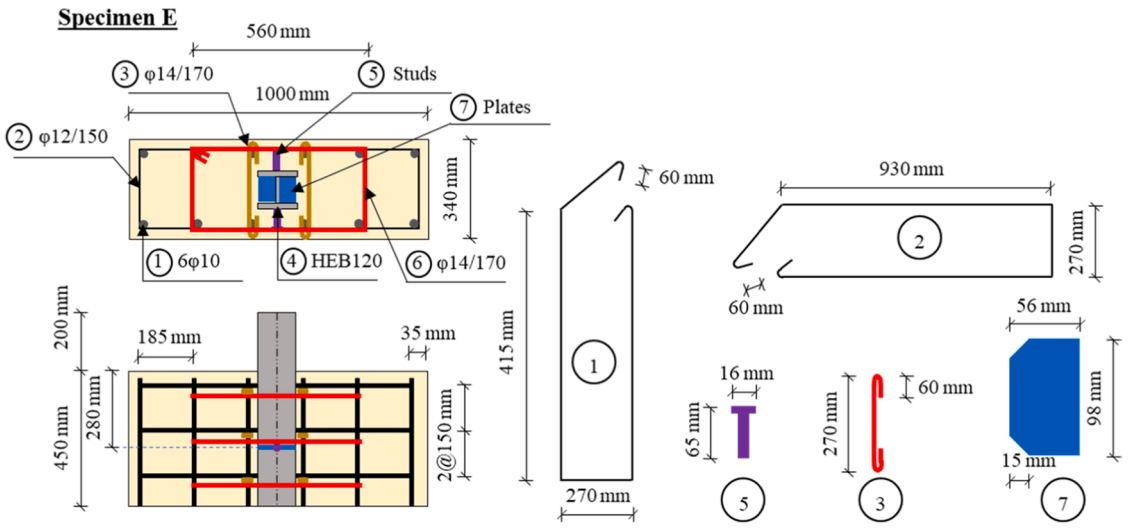

Fig. 7. Configuration E - cross-section detailing.

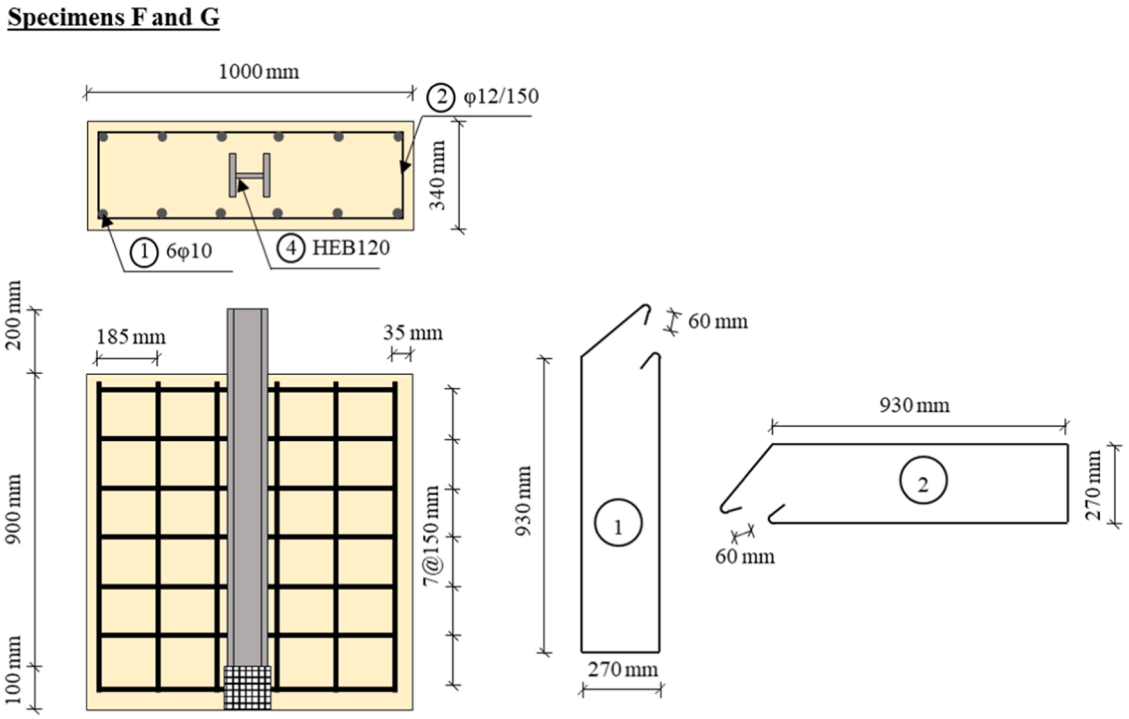

Fig. 8. Configuration F and G - cross-section detailing.

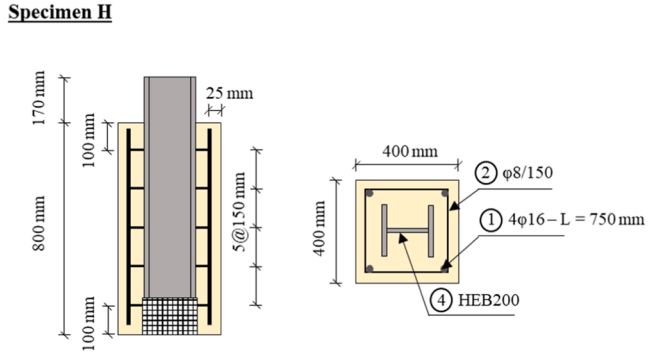

Fig. 9. Configuration H - cross-section detailing.

3.1. Global overview of the experimental campaign

The global load-displacement curves obtained from the tests are shown in Fig. 12a (complete behaviour) and Fig. 12b (up to 1 mm slip for visual clarity on the pre-peak behaviour). Note that, due to the different embedment lengths and geometric dimensions considered for specimens F, G and H, their load-displacement curves are further normalised considering Specimen A as the reference configuration (see Figs. 12c and 12d). A normalisation factor = 0.5 is used for configurations F and G, which is the ratio between the embedment lengths of the profiles in Specimen A and Specimen F (or G). The load-displacement curves for Configuration H (specimens H1, H2 and H3) are normalised with a factor = 0.41, which is obtained by multiplying the ratios between the embedment lengths and perimeters of the different profiles embedded in Specimen A and Specimen H. Fig. 12c and Fig. 12d

Table 1
Steel material properties obtained from the tensile coupon tests (notations correspond to EN ISO 6892–1).

Coupon thickness	Rupture position	S_0	R_{eH}	R_{el}	R_m	$A_{5.65}$		
		(mm^2)	(MPa)	(MPa)	(MPa)	L_0	L_u	A (%)
C1: 8.48 mm	1/2	216.11	455	442	567	85	111.06	30.07
C2: 5.99 mm	1/3	120.32	525	491	622	60	79.77	33.00
C3: 12.11 mm	1/3	242.58	476	446	587	90	116.70	29.70
C4: 6.35 mm	1/2	127.32	501	482	607	65	81.73	25.70

Fig. 10. Preparation of test specimens (a) B3, (b) D2 and (c) E1 before casting.

Fig. 11. Experimental set-up for push-out tests (a) schematic diagram and (b) test set-up and (c) supports.

respectively presents the normalised load-displacement curves corresponding to complete slip and 1 mm slip.

The absolute peak resistance values as well as the resistance values obtained at 1.50 mm slip are also reported (see Table 2). The value at 0.5 mm is considered as a reasonably stabilized post-peak resistance (after bond failure) while the value at 1.5 mm allows, by comparison with the values at 0.5 mm, to evaluate the capacity of the specimens to sustain the load with increasing displacements. Additionally, typical crack patterns are noticed on the longer wall face during the push-out tests on the different specimens – identifying the relevant force-transfer mechanisms and the subsequent failure modes. In general, it is observed that: (i) distinct vertical cracks occur associated to the friction behaviour when the longitudinal shear is transferred through the steel-concrete bond alone, (ii) inclined cracks are noticed when compression struts are formed by the mechanical connectors and (iii) horizontal cracks are observed in presence of horizontal links. Nevertheless, further details regarding the crack patterns are discussed in the following sections with respect to the investigated parameters, along with relevant pictures of the failure modes obtained from the different specimens.

3.2. Analytical assessment of the test specimens

The test specimens are analytically assessed based on the available guidelines of Eurocode 2 [30] and Eurocode 4 [13]. The material properties obtained during the experimental campaign, as discussed in Section 2.2, are considered for the analytical study. All partial safety factors used in the analytical assessment are considered = 1 in order to allow a direct comparison with the experimental results. The plastic design resistance of the profile and the RC wallet are calculated as $N_{pl,\,Rd}$ = 1564 kN and N_{wall} = 13587 kN.

3.2.1. Configurations with shear stud connectors

The resistance provided by each shear stud is estimated based on Eurocode 4 as shown in Eq. 1:

$$P_{Rk} = \min\left(\frac{0.8 \cdot f_u \cdot \pi \cdot \frac{d^2}{4}}{\gamma_V}, \frac{0.29 \cdot \alpha \cdot d^2 \cdot \sqrt{f_{c,exp} \cdot E_{cm}}}{\gamma_V}\right) = \min(72.38\text{kN}, 117.03\text{kN}) = 72.38\text{kN}\ \# \quad (1)$$

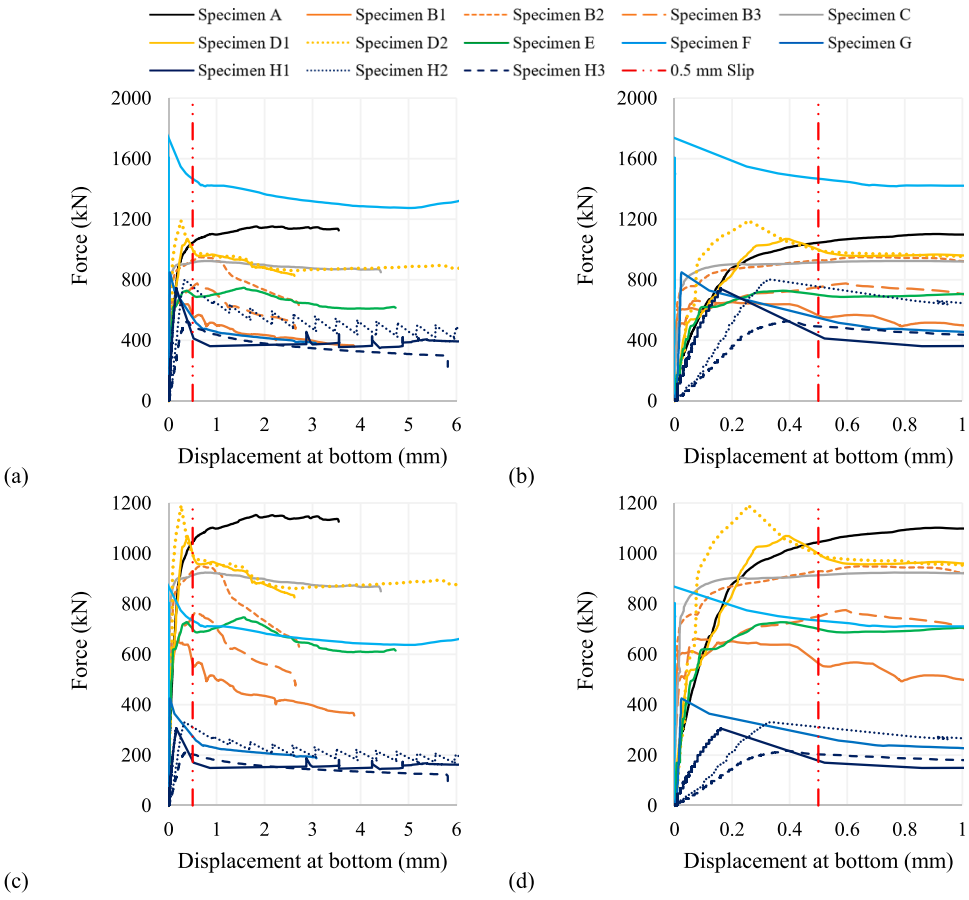

Fig. 12. (a)-(b) Absolute and (c)-(d) normalised load-displacement curves for all specimens using normalization factors for configurations F, G and H, calculated based on the embedment length and perimeter of the profile.

Table 2
Evaluation of resistance at different levels of slip.

Specimen	Peak resistance, $V_{max,\ Exp}$ (kN)	Resistance at 0.5 mm slip, $V_{R\ (0.5),\ Exp}$ (kN)	Resistance at 1.5 mm slip, $V_{R\ (1.5),\ Exp}$ (kN)
A	1150	1050	1130
B1	650	600	450
B2	947	920	800
B3	780	740	605
C	920	910	910
D1	1060	1000	920
D2	1180	1000	950
E	724	700	730
F	1796	1480	1400
G	830	580	420
H*	733	654	484

* The average value is shown for $V_{R(0.5),\ Exp}$ from the 3 specimens (H1, H2, H3).

where, the partial safety factor for shear stud design γ_v is considered equal to 1.00. Therefore, the total shear resistance provided by the 6 shear studs is $V_{Rd,\ Connector} = n_{studs} * P_{Rk} = 434.28$ kN. The horizontal reinforcement scheme for Configuration A and Configuration C is assessed according to the strut and tie model shown in Fig. 13, assuming that the concrete compression struts are formed with an angle $\theta = 45°$.

3.2.2. Configurations with welded plate connectors

The strength of a welded plate connector is determined based on a recently developed design procedure [29] considering the strut & tie model shown in Fig. 14a. The struts are assumed to form at an angle $\theta = 45°$. The strut width is calculated as: $\frac{a}{\cos\theta} = a\sqrt{2} = 80.26mm$. Therefore, the strut resistance can be calculated as:

$$F_{Rd} = a\sqrt{2}\cdot\sigma_{Rd,max}\cdot b = 239.89\text{kN}\# \quad (2)$$

Where $\upsilon' = 1 - \frac{f_{cd}}{250} = 0.716, f_{cd} = f_{c,exp} = 71$MPa (assuming the design safety factor = 1) and $\sigma_{Rd,max} = 0.6\cdot\upsilon'\cdot f_{cd} = 30.5$ MPa. The resistance of a compression strut initiating from a single plate can then be calculated as:

$$V_{Rd,1plate} = F_{Rd}\cdot\cos\theta = 169.62\text{kN}\ \# \quad (3)$$

Therefore, a total no. of 4 plate connectors provide a resistance $V_{Rd,\ Connector} = n_{plates} \times V_{Rd,\ 1plate} = 678.48$ kN.

The bearing thickness of a welded plate is assessed based on the aforementioned design approach [29]. Assuming that the yield lines do not form at 45°, and are hence shorter than $2a\sqrt{2}$ (see Fig. 14b), they can be calculated as: $b\sqrt{2} + a - b/2 = 146.34$ mm. The bearing pressure is calculated as, $w_u = \frac{V_{Rd,1plate}}{A_{plate}} = 31.78$ MPa. Considering $\Phi = 0.9$ and $f_{ay} = 460$ MPa, a 9 mm bearing plate thickness, t_p, is deemed to be sufficient (see Eq. 4). The spacing between two plates is also assessed: $s_{p\_min} = 2a + t_p = 122.5$ mm $\leq s_p = 250$ mm $\leq s_{p\_max} = 6a = 340.5$ mm. The weld thickness, $a = 5$ mm is checked following the condition of $2a > t_p = 9$ mm (see Fig. 14c).

$$t_p \geq \frac{2.8\cdot a}{a + 0.9\cdot b}\sqrt{\frac{2\cdot a^2\cdot w_u\cdot(3\cdot b - 2\cdot a)}{3\cdot\phi\cdot f_{ay}\cdot(6\cdot a + b)}} = 9.02\text{mm} \approx 9\text{mm}\# \quad (4)$$

3.2.3. Configuration with shear studs and plate connectors

Based on the aforementioned values calculated in Sections 3.2.1 and

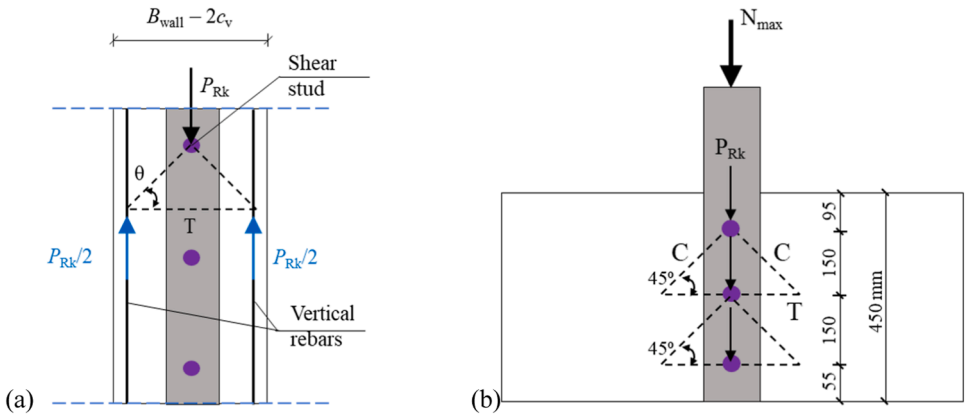

Fig. 13. Strut and tie model used to pre-design (a) Configuration A and (b) Configuration C.

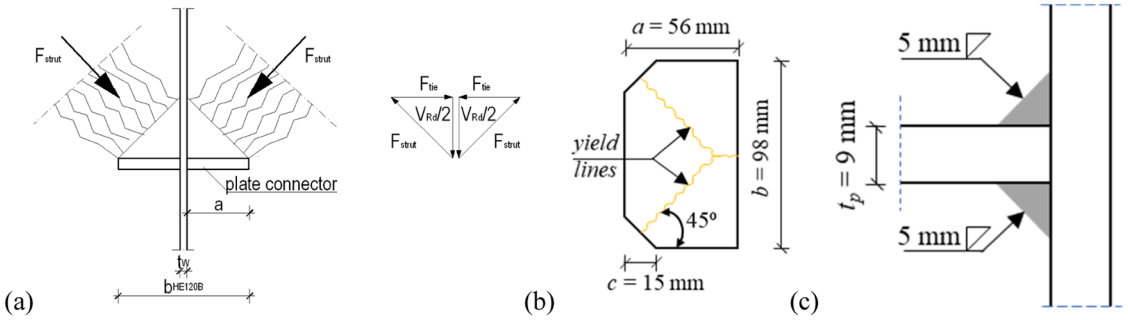

Fig. 14. (a) Strut & tie model to determine plate connector strength, (b) internal bearing plate yield line pattern (fixed condition) and (c) weld dimensions of the plate connector.

3.2.2, a shear connection consisting of 2 studs and 2 plates can theoretically offer a shear resistance, $V_{Rd,Connector} = n_{plates} \cdot V_{Rd,1plate} + n_{studs} \cdot P_{Rk} = 483$kN, provided that they have a compatible deformability. As the shear studs and welded plates are placed orthogonally to each other, their corresponding compression struts are also developing orthogonally to each other and can therefore be assumed to have no significant interaction. The horizontal reinforcement scheme in Configuration E can be assessed following the strut and tie model shown in Fig. 15. The compression struts are assumed to form at an angle, $\theta = 45°$. The tie forces related to each shear stud can be calculated as: $T_1 = \frac{P_{Rk}}{2} = 36.19$ kN and $A_1 = \frac{T_1}{f_{sd}} = 72\text{mm}^2$. The tie forces related to each plate can be calculated as: $T_2 = V_{Rd,1plate} = 169.62$ kN and $A_2 = \frac{T_2}{f_{sd}} = 339$ mm^2. The area of the hoops, placed at a distance, $s_{pc} = 340$ mm, is: $A_{hoop} = A_1 + A_2 = 411$ mm^2.

3.2.4. *Configurations with no mechanical connectors*

The bond resistance in configurations A, B, C, D and E can be evaluated according to Eq. 5 and the design values available in Table 6.6 of Clause 6.7.4.3(3) of Eurocode 4 for completely encased steel sections with a minimum concrete cover and suitable transverse and longitudinal reinforcements.

$$V_{Rd,Bond} = \beta_c \bullet \tau_{Rd} \bullet P \bullet l_e \# \quad (5)$$

where, $\beta_c = 1 + 0.02c_z\left(1 - \frac{c_{z,min}}{c_z}\right) \leq 2.5$; c_z is the nominal concrete cover (= 110 mm for configurations A-E); $c_{z,\,min}$ is the minimum concrete cover (= 35 mm), τ_{Rd} is the design bond stress listed in Table 6.6 of Eurocode 4, P is the perimeter of the embedded steel cross-section, l_e is the embedment length. Therefore, with $\tau_{Rd} = 0.3MPa$, $P = 686$ mm for a HEB 120 profile and $l_e = 450$ mm, the design bond resistance ($V_{Rd,\,Bond}$) can be estimated for configurations A-E as $= 2.5 \bullet 0.3 \bullet 686 \bullet 450/1000 = 232kN$. However, based on the experimental results (discussed later), the bond strength can be assumed zero for Specimen B1 as no horizontal confinement is provided in this case to support the compression struts. On the other hand, the compression struts can develop smoothly in Specimen D1, thanks to the larger space available between the steel and concrete. Therefore, the nominal bond strength can be considered in this case.

According to Table 6.6 of Eurocode 4, for completely or partially encased steel sections with paint, the recommended bond stress is $\tau_{Rd} = 0$ MPa. Information is not available for rusted surfaces. However, for comparison purposes, the design bond stress is assumed to be 0.3 MPa

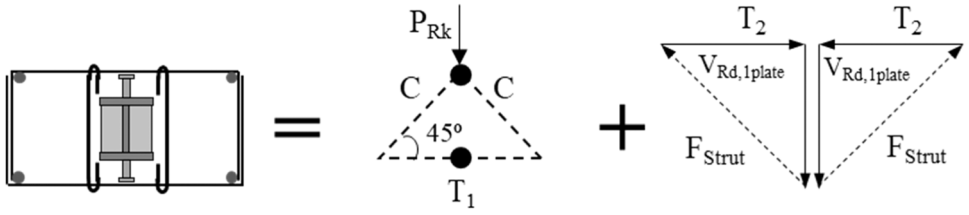

Fig. 15. Calculation of tie forces for a combined shear connection consisting of studs and plates.

Table 3
Resistance to longitudinal shear at steel profile-concrete interface – analytical and experimental.

Spec.	Connect.	Hor. rebars	Web orient.	$V_{Rd,\ Bond}$ (kN)	$V_{Rd,\ Connector}$ (kN)	$V_{Rd,\ Total}$ (kN)	$V_{R(0.5),\ Exp}$ (kN)	$\frac{V_{R(0.5),Exp}}{V_{Rd,Total}}$
A	6 studs	1 link/stud	//	232	434	666	1050	1.57
B1	4 plates	None	//	0	678	678	600	0.88
B2		6 hoops	//	232	678	910	920	1.01
B3		4 links	//	232	678	910	740	0.81
C	6 studs	None	**T**	232	434	666	910	1.37
D1	4 plates	None	**T**	(232)	678	910	1000	1.10
D2		6 links, 6 hoops	**T**	232	678	910	1000	1.10
E	2 studs, 2 plates	6 links, 6 hoops	**T**	232	483	715	700	0.98
F	Rust	None	//	463	0	514	1480	3.19
G	Paint	None	//	0 or 463	0	0 or 514	580	∞ or 1.25
H*	Classic	None	**NA**	561	0	561	654	1.17

*The average value is shown for $V_{R(0.5),\ Exp}$ from the 3 specimens (H1, H2, H3).

(similar to the previous configurations) for both cases. Therefore, with $\tau_{Rd} = 0.3MPa$, $P = 686$ mm for a HEB 120 profile and $l_e = 900$ mm, the design bond resistance ($V_{Rd,\ Bond}$) for configurations F and G is estimated as 463 kN. Similarly, with $P = 1151$ mm for a HEB 200 profile and $l_e = 650$ mm, the design bond resistance ($V_{Rd,\ Bond}$) for Configuration H is estimated as 561 kN. Table 3 summarizes the design analytical resistance of the different specimens V_{Rd} (both for the bond and shear connectors) and compares them with the experimental resistance values obtained at 0.5 mm slip, i.e. $V_{R(0.5),\ Exp}$.

3.3. Influence of the steel profile orientation

The shear studs in specimens A (see Fig. 3) and C (see Fig. 5) are welded to the flanges of the steel profile. The connector plates in specimens B (see Fig. 4) and D (see Fig. 6) are welded in between the flanges of the embedded profile. The orientation of the profile being different for A and C, resp. B and D, it results in a change in the position and distance of the shear studs/plates with respect to the concrete face, and consequently a change in the direction in which the compression struts develop. When the shear studs are placed parallelly to the long wall face (Specimen A) or the plates are placed perpendicularly to the long wall face (Specimen D1), more room is available for the compression struts to develop. On the contrary, the space for compression struts is quite limited when the shear studs are placed perpendicularly to the long wall face (Specimen C) or the plates are placed parallel to the long wall face (Specimen B1). Due to this reason, specimens A and D1 offer a higher resistance compared to specimens C and B1 respectively (see Fig. 16). More cracks are also noticed on the wall face (see Fig. 17) of Specimen C compared to Specimen A and Specimen B1 compared to Specimen D1.

Furthermore, different crack patterns are also noticed in Specimen A (resp. D1) compared to Specimen C (resp. B1) due to the different orientations of the embedded steel profiles. Distinct vertical cracks associated with the friction behaviour appear on the long wall face of specimens A and D1 (see Fig. 17a) as there is no effect of compression struts, whereas, inclined cracks are noticed on the long wall face of specimens C and B1 due to evolution of compression struts (see Fig. 17b). Some general observations can also be made with respect to the values shown in Table 3. The Eurocode 4 design guidelines offer a safe estimation for composite specimens with headed shear studs i.e. configurations A and C, irrespective of the orientation of the steel profile inside the concrete wall, provided a proper transverse tying is implemented. The ultimate resistance obtained from the experiments are found to be 40 % to 50 % greater than the analytical design resistance predicted by Eurocode 4. The deformation capacity is also found to be approximately the same for both specimens.

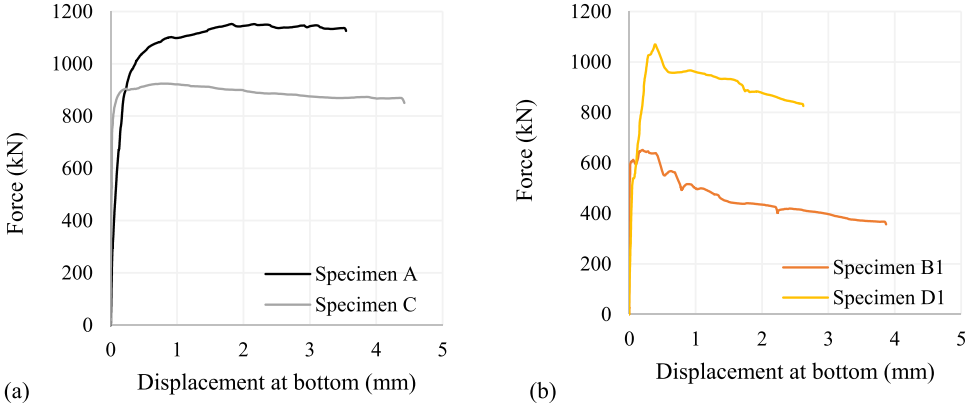

Fig. 16. Comparing the load-displacement behaviour of (a) specimens A and C, (b) specimens B1 and D1.

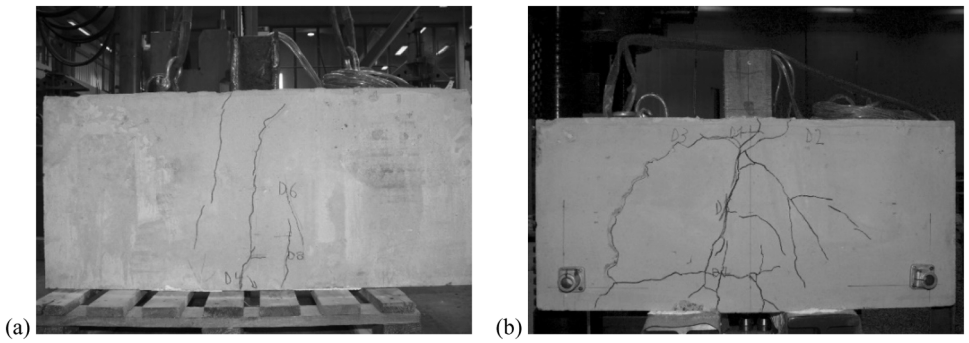

Fig. 17. Cracks obtained on the wall face at failure in (a) Specimen A and (b) Specimen C.

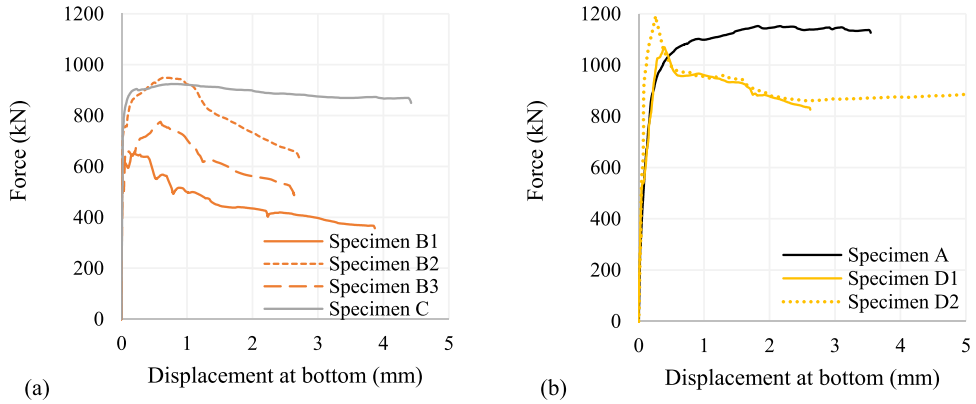

Fig. 18. Load-displacement behaviour of (a) specimens B1, B2 and B3 and (b) specimens D1 and D2.

3.4. *Efficiency of stiffener-like welded plates as stiff shear connectors*

The load-displacement behavior of configurations B and D are compared in Figs. 18a and 18b respectively. Configuration B is also compared with Configuration C, as the compression struts in both these cases develop perpendicularly to the long wall face. Configuration D is compared with Configuration A, where the compression struts develop parallel to the long wall face. The experimental resistances obtained from the three specimens - B2, D1 and D2 (as listed in Table 3), agreed well with the analytical estimations, therefore validating the design of welded plates as shear connectors. Specimens B2 and D2 offer resistances equal to specimens C and A respectively, further encouraging the fact that the welded plate connectors can be used as mechanical connectors to effectively transfer the shear forces at the steel-concrete interface. It should however be noted that such stiff connectors offer lesser deformation capacity compared to the flexible connectors, as shown in Fig. 18. On the contrary, the experimental resistances obtained from the two other specimens, B1 and B3, prove to be insufficient

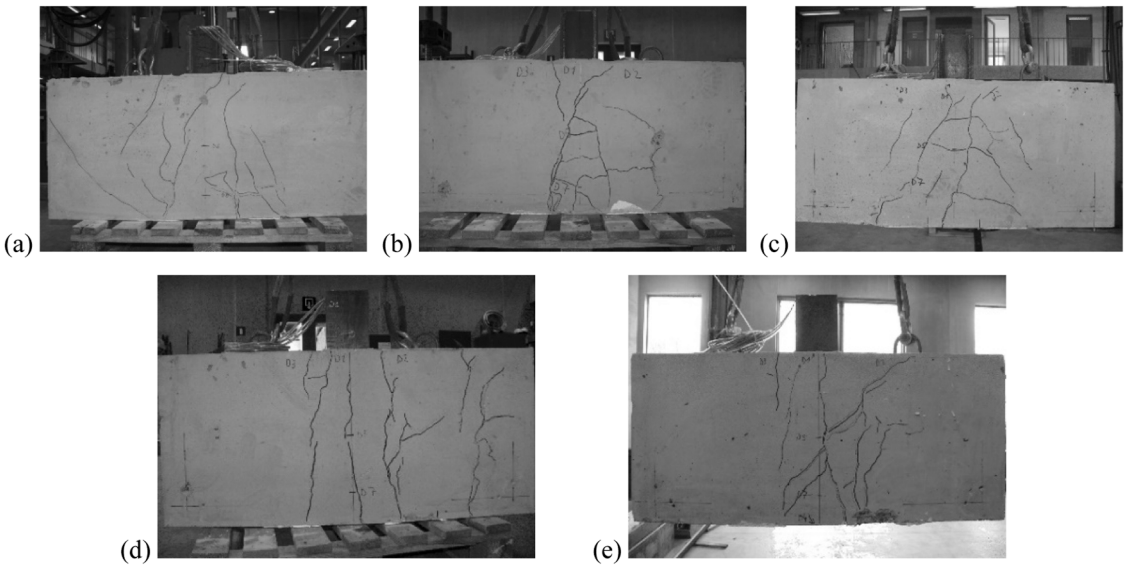

Fig. 19. Crack patterns in specimens (a) B1, (b) B2, (c) B3, (d) D1 and (e) D2.

compared to the analytical calculations. This occurs due to the lack of horizontal confinement and is discussed in the following section. It should also be noted that if sufficient horizontal confinement is provided, Configuration D can provide a better resistance as well as a good deformability compared to Configuration B. This happens due to the same reason stated earlier, namely a limited space restricting the development of compression struts in Configuration B, whereas a larger space allows a smooth progression of compression struts in Configuration D therefore delaying the ultimate failure of the specimen. Fig. 19 presents the crack patterns obtained in specimens B1, B2, B3, D1 and D2 at failure. The horizontal confinement clearly has a significant influence on the crack patterns of the composite specimens and is discussed in the following section.

3.5. Influence of horizontal tying and confining reinforcements

For the configurations with welded steel plate connectors, it can be noticed from Fig. 18a and Table 3 that, when the compression struts are perpendicular to the long wall face (i.e. Configuration B), closed hoops used in Specimen B2 are absolutely necessary to achieve the desired resistance. The experimental resistance obtained in this case is almost perfectly predicted by the analytical calculations. On the other hand, confinement by links connecting the mesh, as used in Specimen B3, proves to be less effective as the experimental resistance is obtained as 740 kN instead of an analytically calculated resistance of 910 kN. Specimen B1 performs worse as no horizontal confinement is provided in this case to support the compression struts. Only 600 kN resistance is achieved from the test, which is lower than the connector strength, let alone the combined strength estimated from the bond and the connectors. Therefore, it can be stated that the horizontal confinement plays an important role in controlling the failure mode of the composite specimen where the embedded profile is oriented with its strong axis perpendicular to the longer wall face and welded plate connectors are used. On the contrary, Fig. 18b shows that when compression struts are parallel to the long wall face (i.e. Configuration D), the same resistance could be obtained with or without horizontal confinement. Specimens D1 and D2 both provide an equal experimental resistance at 0.5 mm slip, $V_{R(0.5),\,Exp}$ = 1000 kN, being 1.1 times more than the analytical prediction. This happens because, in these cases, the compression struts have more volume of concrete to spread into and therefore can find steady anchorage in the steel meshes parallel to the longer faces of the wall. Comparing Table 3 and Fig. 18b, it can also be noticed that the adopted design approach for shear transfer through welded plate connectors provides a safe estimate of the resistance value compared to the experimental resistance. Although, the horizontal confinement can slightly increase the stiffness and the peak resistance, they do not seem to have a significant influence in these cases. However, the horizontal confinement is observed to have a direct influence on the crack pattern of the composite specimens. Distinct inclined cracks occur in B1 solely due to the compression struts developing perpendicular to the wall. On the other hand, clear vertical cracks are noticed for D1, associated with pure friction. No horizontal cracks are obtained in these cases due to the absence of horizontal links. On the other hand, major horizontal cracks are seen in B2, B3 and D2 due to the horizontal links/hoops, along with inclined cracks in B2 and B3, and vertical cracks in D2.

3.6. Combination of different types of shear connectors and bond strength

Eurocode 4, as well as other standards, does not provide a specific clause to combine the design longitudinal shear strengths coming from different types of shear connectors and/or the frictional resistance at steel-concrete interface. The available state-of-the art research studies however indicate that friction resistance and mechanical interaction, both of which being potentially associated with consistent slip displacement, could be combined to resist the longitudinal shear at a steel-concrete interface. The push-out test on Specimen E (Fig. 7) can be used as an example to further validate this hypothesis. While the previously discussed configurations (A, B, C and D) are designed and constructed with only one type of shear connector (flexible or stiff), Configuration E is designed with both shear studs and welded plates. Fig. 20 presents the load-displacement behaviour and crack pattern of Specimen E obtained from the experiments. Firstly, comparing the analytical and experimental values (see Fig. 20 and Table 3), it can be stated that, adding the resistance of the studs with the resistance offered by the plate connectors and the steel-concrete bond provides a good estimate of the real strength. Secondly, a comparison between the load-displacement behaviour of Specimen E (having 2 studs and 2 plates) with the load-displacement behaviours (scaled with respect to the number of mechanical connectors) obtained from Specimen C (6 studs) and Specimen D2 (4 plates) confirms that an approximately equal shear strength can be achieved by combining two types of mechanical connectors. Therefore, the Eurocode 4 provisions can be safely used along with the design approach adopted for the welded plate connectors (Section 3.2), in order to combine them with the bond strength. Appropriate safety factors should however be considered before real-life design applications.

The previously discussed specimens (Configurations A-D) are also analysed further to check if a safe prediction can be obtained regarding their ultimate resistance, by combining the shear strength provided by the mechanical connectors and the friction resistance provided by the steel-concrete bond. Based on the analytical and experimental results, it can be stated that the provisions of Eurocode 4 can be safely applied to obtain the combined shear strength for the configurations with shear stud connectors (i.e. A and C), independently of the orientation of the steel profile. The analytical values of the shear strength in these cases prove to be significantly lesser than the experimental values, validating

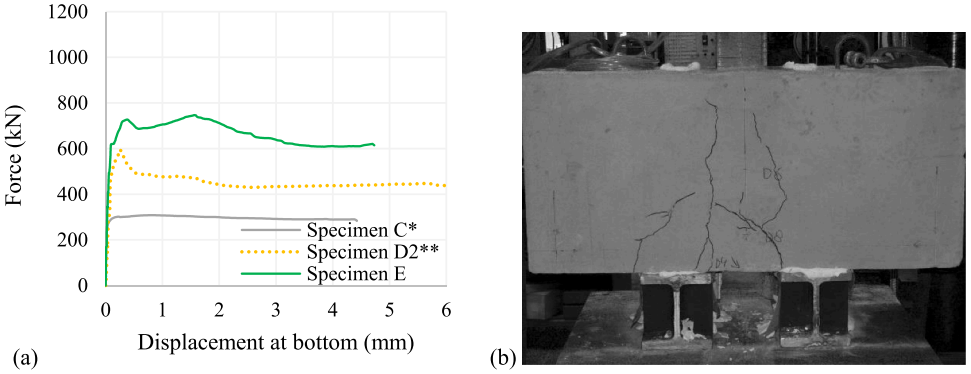

Fig. 20. (a) Comparing the load-displacement behaviour between specimens E, C* (representing the scaled load-displacement behaviour of Specimen C with a factor = 1/3) and D2 * * (representing the scaled load-displacement behaviour of Specimen D2 with a factor = 1/2) and (b) cracks obtained at failure for Specimen E.

a safe and practical approach. However, the same cannot be stated for the configurations with welded plate connectors (i.e. B and D). In these cases, combining the steel-concrete bond strength with the connector strength serve as a safe approach if either of these two choices are ensured: (i) necessary horizontal confinement is provided (as done in Specimen B2) or (ii) sufficient concrete volume is provided for a smooth progression of the compression struts (as done in Configuration D1 and D2). If none of these solutions are implemented, a summation of the bond strength and the plate connector resistance can lead to an over-estimated connection strength and therefore an unsafe shear connection between the steel and concrete.

3.7. Influence of different steel-concrete material condition on the bond component

The load-displacement behaviours and the bond stress-slip results, realised from specimens F, G and H are respectively shown in Fig. 21 and Fig. 22. Important information can be derived regarding the different types of surface finishing used on the steel profile embedded into the concrete sections, i.e. (i) an artificially rusted surface in Specimen F, (ii) smoothly painted surface in Specimen G and (iii) a surface without specific finishing in Specimen H.

As discussed in Section 3.2.4, the bond resistance at the steel concrete interface can be calculated using the perimeter of the embedded profile and its embedded length inside the concrete section. Similarly, we can determine the bond stress by dividing the resistance values ($V_{R\,(0.5),\,Exp}$ in Table 3) obtained from the tests by the two foretold parameters. For specimens F and G, the embedded HEB 120 profile has a perimeter = 686 mm and an embedment length, $l_{embHEB120} = 900$ mm. The $V_{R(0.5),\,Exp}$ is obtained as 1480 kN and 580 kN respectively for specimens F and G. Therefore, the bond strength offered by the rusted specimen, i.e. Configuration F, can be calculated as: $\tau_{R,\,exp} = 1480$ kN / 0.617 m^2 = 2.39 N/mm^2; which is almost 3 times greater than the design value obtained from the Eurocode 4 recommendations: $\beta c \times \tau_{Rd} = 2.5 \times 0.3 = 0.75$ N/mm^2. Even if we consider a partial safety factor of 1.25, the estimated design strength can be obtained as: $1.25 \times 0.75 = 0.94$ N/mm^2, which is still 60 % lower than the experimental value. Such observations actually indicate that the basic τ_{Rd} value (= 0.3) recommended by Eurocode 4 may cause great underestimation for fully encased steel profiles with artificially rusted surfaces. Similarly, the bond strength offered by the painted specimen, Configuration G, can be derived as: $\tau_{R,\,exp} = 580$ kN / 0.617 m^2 = 0.93 N/mm^2. Although Eurocode 4 indicates that nothing reliable can be stated if there is paint or loose rust or grease on the surface of the embedded steel profile and does provide a "zero" design value ($\tau_{Rd} = 0$) for such cases, the values obtained from the experiments are not at all insignificant. It can even be seen that the bond strength obtained while using anti-rust paint is actually greater than the basic Eurocode 4 design value: $\beta c \times \tau_{Rd} = 2.5 \times 0.3 = 0.75$ N/mm^2. Therefore, further design values are

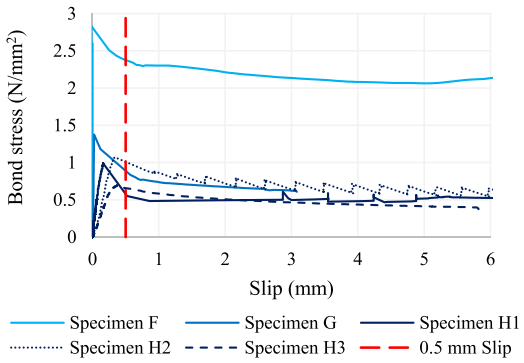

Fig. 22. Bond stress-slip behaviour of specimens F, G, H1, H2 and H3.

necessary to characterize and optimize the bond stresses for completely encased steel sections with paint or rust in addition to the design values already available in Table 6.6 of Clause 6.7.4.3(3) of Eurocode 4. A value of 0.2 was recommended by Roeder et al. [16] for encased steel sections with paint, which seems to be a reasonable estimate. Finally, the bond stress in Configuration H can be calculated corresponding to an average value of $V_{R(0.5),\,Exp} = 654$ kN, obtained from the 3 tested specimens. The external perimeter of an HEB200 section is 1151 mm and the bond resistance can be calculated considering the full embedment length of the profile, $l_{embHEB200} = 650$ mm. Therefore, the bond strength offered by the classical specimen can be estimated as: $\tau_{R,\,exp}$ = 654 kN / 0.520 m^2 = 0.87 N/mm^2 [31]. This value further confirms the safe yet conservative nature of the Eurocode 4 in determining the bond strength at steel-concrete interfaces. Fig. 23 presents the crack patterns obtained in configurations F and G at the time of failure. When the load was applied and the steel profile started sliding through the concrete, distinct vertical cracks started to form on the long wall face along the length of the embedded profile, associated with pure friction which eventually leads to expansion of the concrete surrounding the profile.

The evolution of axial load along the embedded steel profile ($N_{profile}$) is plotted in Fig. 24a and Fig. 24b, respectively for specimens F and G, as a percentage of the total axial load applied at the top of the composite specimens ($N_{applied}$). $N_{profile}$ is calculated by multiplying the young's modulus and the cross-section area of the embedded steel profile with the strain values obtained from the strain gauges placed along the embedment length of the steel profile. 4 load levels are chosen to characterize the load evolution – 25 %, 50 %, 75 % and 90 % of the maximum resistance ($V_{max,\,Exp}$ values listed in Table 2) obtained from the tests corresponding to each specimen. The position of the strain gauges (90 mm, 240 mm, 390 mm, 540 mm, 690 mm and 840 mm) are measured from the top of the wall. The bottom most strain gauge results for Specimen G could not be obtained due to installation errors and are

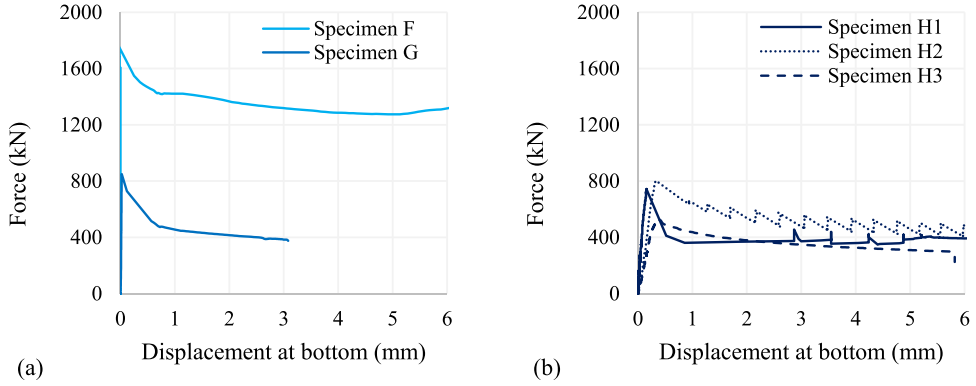

Fig. 21. Absolute load-displacement behaviour of (a) specimens F and G (b) specimens H1, H2 and H3.

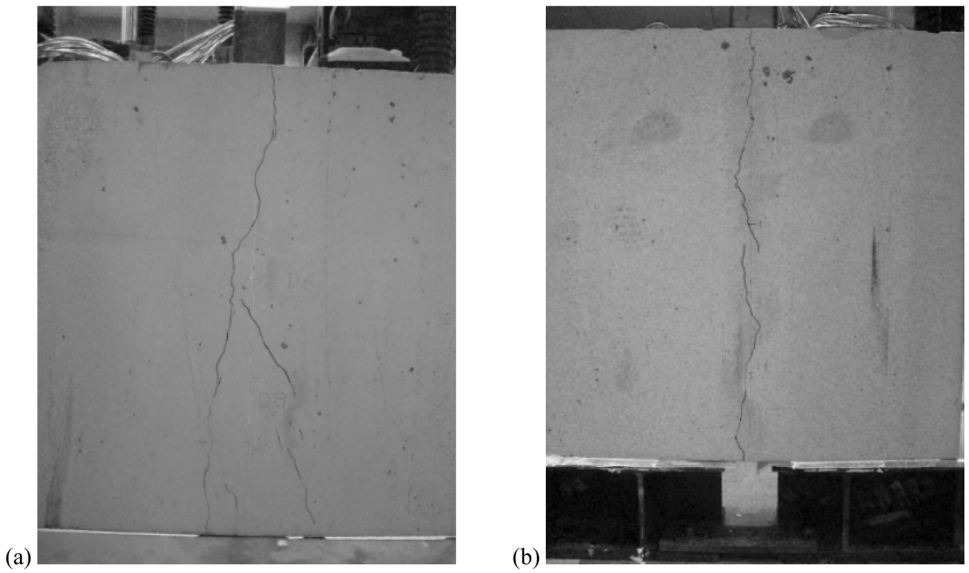

Fig. 23. Crack patterns observed during failure of (a) Specimen F and (b) Specimen G.

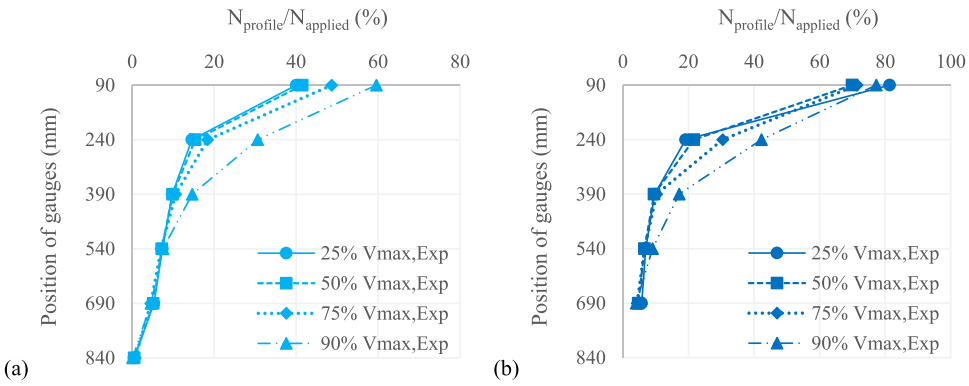

Fig. 24. Evolution of axial loads along the steel profile embedded in (a) Specimen F and (b) Specimen G.

therefore not plotted in Fig. 24. A realistic and expected evolution of axial load can be observed confirming an effective force-transfer till the bottom of the specimen. Furthermore, the profile in Specimen G is observed to take a higher percentage of the applied axial load compared to Specimen F. This happens due to the fact that the rusted surfaces of the embedded profile in Specimen F provides a larger bond strength and therefore is able to transmit the applied load to the surrounding concrete in a better way compared to the painted surface used in Specimen G.

4. Conclusions

This research paper investigates the transfer of the longitudinal shear between an embedded profile and the surrounding concrete for different configurations of the shear connection through push out tests. A specific feature of the tests performed is the non-symmetrical shape (i.e. rectangular) of the concrete block creating important differences in function of the orientation of the profile. The final aim of this research is to identify suitable solutions in the perspective of using profiles as reinforcement in concrete walls. Different types of shear connectors, horizontal reinforcement schemes and orientation of the steel profile are investigated in order to characterize the shear strength behaviour at the steel-concrete interface in accordance to the structural codes, especially Eurocode 2 and 4. The Eurocode 2 and 4 provisions are directly applicable for the specimens having shear stud connectors, while a newly developed design approach, based on an appropriate strut and tie mechanism, is considered for specimens with welded steel plate connectors.

Relevant conclusions could be drawn from the analytical and experimental investigations. For instance, it is observed that Eurocode 4 offers a safe approach to calculate the longitudinal shear resistance of composite specimens with shear stud connectors as well as the bond strength offered by the steel-concrete interface. The stiffener-like steel plates are able to provide an adequate amount of shear strength to the steel-concrete interface and can therefore be deemed as a viable alternative to the shear studs. A method relying on strut and tie mechanisms, as adopted in this study, can be used to design them in an efficient manner. However, it should be noted that, the welded steel plates work as “rigid” shear connectors and offer less deformation capacity compared to the “flexible” shear stud connectors. The orientation of the embedded steel profile, consequent position of the stud or plate connectors and the distance to the concrete face define the possible development of the compression struts, which as a result dictates the necessity or not of horizontal confinement or ties. Limited distance between the connector and the concrete face restricts the development of compression struts, leading to lower strength and early failure of the steel-concrete interface. On the contrary, a larger distance allows the full development of the struts. However, if suitable horizontal confinement or tying is adopted, the Eurocode 4 guidelines or the proposed strut and tie approach offer a conservative approach to respectively design the stud/welded plate connection irrespective of the orientation of the

profile. It is also observed that two different types of shear connectors can be combined by simply adding their resistances to obtain the total resistance of the steel-concrete interface against longitudinal shear, provided that the necessary horizontal tying (depending on the profile orientation, type of connectors, concrete cover etc.) is implemented in order to bring the compression struts in equilibrium by steel bars acting in tension. Similarly, contributions to the shear resistance provided by the direct bond and by the adopted connectors can be added to achieve the necessary longitudinal shear resistance, provided that the necessary horizontal confinement is considered (i.e. to increase the compression resistance and prevent lateral expansion of concrete) based on the profile orientation, type of connectors, concrete cover etc. However, additional design values would be useful to characterize and further optimize the bond strength for completely encased painted or rusted steel sections, in addition to the design values already available in Table 6.6 of Clause 6.7.4.3(3) of Eurocode 4. To that purpose, detailed numerical studies are currently being conducted using finite element models, calibrated based on the tests results discussed in this article.

Funding

Part of this research was funded by the Research Fund for Coal and Steel of the European Commission, Research grant agreement RFSR-CT-2012–00031.

CRediT authorship contribution statement

Herve Degee: Conceptualization, Funding acquisition, Methodology, Resources, Supervision, Writing – review & editing. **Teodora Bogdan:** Investigation, Methodology, Writing – review & editing. **Rajarshi Das:** Data curation, Investigation, Validation, Writing – original draft. **Dan Dragan:** Data curation, Investigation, Software, Writing – review & editing.

Declaration of Competing Interest

The authors declare that they have no known competing financial interests or personal relationships that could have appeared to influence the work reported in this paper.

Data availability statement

The data presented in this study are available on request from the corresponding author. The data are not publicly available due to the fact that it is part of an ongoing research.

Acknowledgement

This paper was developed in the frame of the SMARTCOCO project funded by RFCS, the Research Fund for Coal and Steel of the European Commission, Research grant agreement RFSR-CT-2012–00031 Smartcoco. The companies BESIX and ArcelorMittal are also acknowledged for their contribution and involvement in the project.

References

[1] Wallace J.W., Orakcal K., Cherlin M., Sayre B.L. Lateral-load behavior of shear walls with structural steel boundary columns. Proceedings of Sixth ASCCS Conference on Composite and Hybrid Structures, Los Angeles, USA; 2000. p. 801–808.
[2] Qian J, Jiang Z, Ji X. Behaviour of steel tube-reinforced concrete composite walls subjected to high axial force and cyclic loading. Eng Struct 2012;36(3)):173–84.
[3] Ji X, Sun Y, Qian J, Lu X. Seismic Behaviour and modelling of steel reinforced concrete (SRC) walls. Earthq Engng Struct Dyn 2015;44:955–72.
[4] Zhou Y, Lu X, Dong Y. Seismic behaviour of composite shear walls with multi encased steel sections. Part 1: experiment. The structural design of tall and special buildings. Wiley Online Library,; 2010. p. 618–36.
[5] Dan D, Fabian A, Stoian V. Theoretical and experimental study on composite steel–concrete shear walls with vertical steel encased profiles. J Constr Steel Res 2011; 67:800–13.
[6] Dan D, Fabian A, Stoian V. Nonlinear behavior of composite shear walls with vertical steel encased profiles. Eng Struct 2011;33:2794–804.
[7] Dan D, Fabian A, Stoian V. Numerical investigation on the effect of axial force to the behaviour of composite steel concrete shear walls. 8th Int Conf Behav Steel Struct Seism Areas Shanghai, China 2015 July:1–3.
[8] AISC Standard 341–10. Seismic provisions for structural steel buildings. Chicago, IL: American Institute of Steel Construction; 2010.
[9] Eurocode 8: Design provisions for earthquake resistance - part 1: general rules, seismic actions and rules for buildings. Brussels: European Committee for Standardization; 2004.
[10] JGJ 3–2010. CMC. Technical specification for concrete structures of tall building (JGJ 3–2010). Beijing: China Ministry of Construction; 2011.
[11] Salari MR. Modeling of bond-slip in steel-concrete composite beams and reinforcing bars. University of Colorado; 1999.
[12] Daniels BJ, Crisinel M. M. Composite slab behavior and strength analysis. Part II: Comparisons with test results and parametric analysis. J Struct Eng 1993;119(1): 36–49.
[13] Eurocode 4 (2004). EN 1994–1-1: Design of composite steel and concrete structures, part 1.1– general rules for buildings. Brussels: European Committee for Standardizations; 2004.
[14] Hawkins N, Mitchell D. Seismic response of composite shear connections. J Struct Eng 1984;110(9):2120–36.
[15] Viest I, et al. Composite construction design for buildings. McGraw-Hill; 1997.
[16] Roeder C, et al. Shear connector requirements for embedded steel sections. J Struct Eng 1999;125(2):142–51.
[17] Hawkins N. Strength of concrete encased steel beams. Institution of Engineers (Australia); Civil Eng Trans 1973; CE15(1–2): 29–45.
[18] Hamdan M. and Hunaiti Y. Factors affecting bond strength in composite columns. 3rd Int. Conf. on Steel-Concrete Composite Structures, Fukuoka, Japan, 1991.
[19] Wium J, Lebet J. Force transfer in composite columns consisting of embedded HEB 300 and HEB 400 sections. Éc Polytech Fed, Lausanne, Switz 1992.
[20] Lungershausen H. Zur Schubtragfähigkeit von Kopfbolzendübeln, Institut für Konstruktiven Ingenieurbau, Ruhr-Universität, 1988.
[21] Johnson RP, Oehlers DJ. Analysis and design for longitudinal shear in composite T-beams. Proc Inst Civ Eng 1981;71(2):989–1021.
[22] Oehlers D, Johnson R. The strength of stud shear connections in composite beams. Struct Eng 1987;65(2):44–8.
[23] Oehlers D, Park S. Shear connectors in composite beams with longitudinally cracked slabs. J Struct Eng 1992;118(8):2004–22.
[24] Oehlers DJ. Development of design rules for retrofitting by adhesive bonding or bolting either FRP or steel plates to RC beams or slabs in bridges and buildings. Compos Part A: Appl Sci Manuf 2001;32(9):1345–55.
[25] Ali M, et al. Shear peeling of steel plates bonded to tension faces of RC beams. J Struct Eng 2001;127(12):1453–9.
[26] Chen J, Teng J. Anchorage strength models for FRP and steel plates bonded to concrete. J Struct Eng 2001;127(7):784–91.
[27] Rabbat B, Russell H. Friction coefficient of steel on concrete or grout. J Struct Eng 1985;111(3):505–15.
[28] Degee H., Plumier A., Mihaylov B., Dragan D., Bogdan T., Popa N., et al. Smart Composite components – concrete structures reinforced by steel profiles "SmartCoCo"; 2016.
[29] Plumier A, et al. ISBN 9780367712075. Design of Hybrid Structures – where Steel Profiles meet Concrete. 1st edition.,. Routledge, Taylor & Francis Group,; 2023.
[30] Eurocode 2 (2004). EN 1992–1-1: Design of concrete structures, part 1.1 – general rules for buildings. Brussels: European Committee for Standardizations; 2004.
[31] Bogdan T., Degee H., Dragan D., Obiala R., Shear transfer at the steel-concrete interface using different mechanical connectors, 10th Eurosteel Conference, 2023; September 12–14, Amsterdam, The Netherlands.